UCRL-1637

UNIVERSITY OF CALIFORNIA — BERKELEY

TWO-WEEK LOAN COPY

This is a Library Circulating Copy which may be borrowed for two weeks. For a personal retention copy, call Tech. Info. Division, Ext. 5545

RADIATION LABORATORY

UCRL-1637 c.2

DISCLAIMER

This document was prepared as an account of work sponsored by the United States Government. While this document is believed to contain correct information, neither the United States Government nor any agency thereof, nor the Regents of the University of California, nor any of their employees, makes any warranty, express or implied, or assumes any legal responsibility for the accuracy, completeness, or usefulness of any information, apparatus, product, or process disclosed, or represents that its use would not infringe privately owned rights. Reference herein to any specific commercial product, process, or service by its trade name, trademark, manufacturer, or otherwise, does not necessarily constitute or imply its endorsement, recommendation, or favoring by the United States Government or any agency thereof, or the Regents of the University of California. The views and opinions of authors expressed herein do not necessarily state or reflect those of the United States Government or any agency thereof or the Regents of the University of California.

UCRL-1637
Unclassified Physics Distribution

UNIVERSITY OF CALIFORNIA

Radiation Laboratory

Contract No. W-7405-eng-48

NEUTRAL MESON GAMMA SPECTRA FROM PROTON BOMBARDMENT OF CARBON

Walter Ellis Crandall
(Thesis)

January 8, 1952

Berkeley, California

CONTENTS

I.	INTRODUCTION	3
II.	THEORY	5
III.	GENERAL ARRANGEMENT AND PROCEDURE	9
IV.	SPECTROMETER ANALYSIS	10
	A. Quadruple Coincidence Circuit	10
	B. Geiger Coincidence Matrix	10
	C. Detection Efficiency of the Converted Gamma Rays	11
	D. Mean Energy of Matrix Channels	12
	E. Loss of Energy of Electrons in Radiator	14
	F. Multiple Scattering in Radiator	14
V.	PROTON BEAM MONITOR	16
VI.	RESULTS AND CONCLUSIONS	17
VII.	ACKNOWLEDGEMENTS	23
VIII.	REFERENCES	24
IX.	FIGURES	27

NEUTRAL MESON GAMMA SPECTRA FROM PROTON BOMBARDMENT OF CARBON

Walter Ellis Crandall

Radiation Laboratory, Department of Physics
University of California, Berkeley, California
January 8, 1951

I. INTRODUCTION

Yukawa[1] in 1935 postulated a particle with a mass intermediate between that of the electron and the proton to explain the short range nuclear forces. This particle, which he called a meson, necessarily interacted strongly with matter. Therefore, when highly penetrating particles were observed in cosmic radiation which appeared to interact weakly with matter, it was difficult to interpret these particles as a confirmation of the theory. Lattes, Occhialini, and Powell[2], in a study of photographic plates exposed to cosmic radiation at high altitudes, first found evidence for mesons which interacted strongly with nuclei to form stars and, in addition, many of these particles were observed to decay into mesons which interacted weakly with matter and presumably formed the bulk of the penetrating radiation observed at lower altitudes. Cosmic ray experiments accumulated considerable data which in their complexity were difficult to analyze into precise conclusions as to the fundamental properties of the mesons, primarily due to the complete randomness in energy and time of the events observed.

It was not until mesons could be produced in the laboratory that the fundamental properties of these particles could be classified. The strongly interacting positive and negative mesons, called pions by Fermi[3], were found to have a rest energy of 140 ± 1.5 Mev[4,5] and a mean lifetime of about 2×10^{-8} seconds[6,7]. The charged pion decays into a neutrino and the corresponding charged muon, the weakly interacting meson, with a rest

energy of 107 ± 1.2 Mev[4] and a mean lifetime of about 2×10^{-6} seconds[8]. The muon finally decays into two neutrinos and an electron. These decay processes are in competition with capture of the meson by nuclei with the consequent emission of photons or the disruption of these nuclei with the emission of neutrons, protons, deuterons and heavier mass fragments.

The properties of the charged mesons fit well into the complex picture of cosmic ray events, but an excessive electronic component observed in primary showers in the upper atmosphere seemed difficult to explain by their properties alone. Oppenheimer[9], Marshak[10] and others proposed a neutral pion decaying into two gamma rays to explain the electron component. Moyer and York[11] first observed that high energy gamma radiation emitted from targets bombarded by protons in the Berkeley synchrocyclotron fit the hypothesis of a neutral pion decaying into two gamma rays. Panofsky, Steinberger and Stellar[12] found correlated pairs of gamma rays emitted from targets bombarded by x-rays from the 320 Mev synchrotron. This was followed by Panofsky, Aamodt and Hadley's[5] observation of gamma radiation originating from radiative capture of negative pions and the resulting decay radiation. This experiment assigned a precise rest energy for the negative pion of 140 ± 1.3 Mev and also the mass difference between the negative pion and neutral pion of 5.4 ± 1.0 Mev and, in addition, placed severe restrictions on the parity and spin of the pions.

The lifetime of the neutral pion is extremely short as shown in a study by Carlson, Hooper and King[13] of electron pairs close to nuclear explosions in photographic plates exposed at high altitudes. This study not only confirmed the neutral pion hypothesis, but it also set an upper limit on the neutral pion lifetime of less than 5×10^{-14} seconds. An

experiment reported on in this paper also places an upper limit of less than 10^{-12} seconds.

The bulk of this paper will be concerned with the precise form of the gamma ray spectra emitted by carbon tragets bombarded by protons in the Berkeley cyclotron, and the excitation function for this radiation. In addition the distribution of the neutral pions emitted by the target is inferred from the averaged gamma ray spectrum.

II. THEORY

Carlson, Hooper and King[13] have derived expressions for the gamma ray spectra from the decay of neutral pions which are useful in interpreting the data reported on in this paper.

If it is assumed that a neutral pion in its rest frame decays into two gamma rays of energy K_o distributed spherically symmetrically, then in any other frame,

$$K = \frac{K_o}{\gamma(1 - \beta \cos \theta)} = K_o \; \gamma(1 + \beta \cos \alpha) \tag{1}$$

and

$$\cos \theta = \frac{\beta + \cos \alpha}{1 + \beta \cos \alpha} \tag{2}$$

where α is the angle in the rest frame between the photon direction and the neutral pions direction and θ is the corresponding angle in a reference frame for a neutral pion moving with velocity β. (See Fig. 1) The angular variation in intensity of the gamma radiation due to a monoenergetic beam of neutral pions is then

$$I(\theta) = \frac{dN}{d\Omega} = \frac{dN}{d\Omega_o} \frac{d\Omega_o}{d\Omega} = \frac{d \cos \alpha}{d \cos \theta} \; Io \tag{3}$$

Which from (2) gives

$$I(\Theta) = \frac{I_o}{\gamma^2 (1 - \beta \cos \Theta)^2} \tag{4}$$

Since K is a function of Θ alone for the case of a monoenergetic neutral pion beam we may write

$$n(K)\, dK = 1/2\, I(\Theta) \sin \Theta d\Theta \tag{5}$$

and using (1) and (4) we find

$$n(K) = \frac{I_o}{2\beta\gamma K_o} = \frac{I_o}{\sqrt{E^2 - E_o^2}} \tag{6}$$

for

$$\gamma Ko(1 - \beta) \leq K \leq \gamma Ko(1 + \beta) \tag{7}$$

and

$$n(K) = 0 \tag{8}$$

outside the limits in (7).

For the case of an inhomogeneous beam of neutral pions, F(E)dE between E and E + dE, the gamma ray intensity would be

$$n^1(K) = \frac{2F(E)dE}{2\beta\gamma K_o} = \frac{2F(E)dE}{\sqrt{E^2 - E_o^2}} \tag{9}$$

for the limits given by (7)

$$E - \sqrt{E^2 - 4K_o^2} \leq 2K \leq E + \sqrt{E^2 - 4K_o^2} \tag{10}$$

The total gamma ray intensity, N(K) is found from (9) by integrating over all energies capable of producing a gamma ray of energy K.

$$N(K) = \int_{\frac{K^2 + K_o^2}{K}}^{\infty} \frac{2F(E)\, dE}{\sqrt{E^2 - E_o^2}} \tag{11}$$

where the lower limit of integration is obtained from the limits of (10). If we differentiate (11) we find

$$F\left(\frac{K^2 + K_o^2}{K}\right) = \frac{-K}{2} \frac{dN(K)}{dK} \tag{12}$$

and this allows us to find the distribution in energy of the neutral pions if we once know the total gamma ray spectrum from the decay of the neutral pion. All angular dependence has been removed from this equation since we assume that N(K) is the total gamma ray intensity for all angles of emission from the target.

If we consider a gamma ray spectrum that is axial symmetric in frame Σ' but otherwise is a function of Θ' and K'.

$$I'(K'\Theta') = \frac{dN'(K'\Theta')}{dK'd\Omega'} \tag{13}$$

In any other reference frame

$$I(K\Theta) = \frac{dN(K'\Theta')}{dK'd\Omega'} \frac{dK'}{dK} \frac{d\Omega'}{d\Omega} \tag{14}$$

and using relations similar to (1) and (2)

$$I(K\Theta) \cong \frac{I'(K'\Theta')}{\gamma(1 - \beta \cos \Theta)} \tag{15}$$

and

$$K = \frac{K'}{\gamma(1 - \beta \cos \Theta)} \tag{16}$$

Thus we see that I and K both transform by the same factor and, for the case of spherically symmetric emission of gamma radiation in any frame, Σ'',

$$I''(K''\Theta'') = I''(K'') \tag{17}$$

In this case all gamma ray spectra for any angle of view in any reference frame will be identical in shape when log I is plotted against log K.

To illustrate the properties of the gamma ray spectrum from another point of view let us consider a monoenergetic spherically symmetric source of neutral pions. Formula (6) shows that the gamma ray spectrum would be a step function as shown in Fig. 2 with the geometric mean of the extreme energies equal to half the neutral pion rest energy and with the area under the curve equal to twice the number of neutral pions. Since the neutral pions are not monoenergetic the actual spectrum is a

summation of such step functions with different extremes but the same geometric mean as shown in Fig. 2. Then the neutral pion energy distribution is related to the gamma ray spectrum through the area in each step.

$$F(E)\Delta E = \frac{\Delta A}{2} = -\frac{(K_{max} - K_{min})\Delta N}{2} \tag{18}$$

where

$$K_{max} K_{min} = K_o^2 \tag{19}$$

and from (10)

$$F(E) = 1/2 \frac{\Delta N}{\Delta E}\sqrt{E^2 - E_o^2} \tag{20}$$

or

$$F(E) = \frac{-K_{max}}{2} \frac{\Delta N}{\Delta K_{max}} = \frac{-K_{min}}{2} \frac{\Delta N}{\Delta K_{min}} \tag{21}$$

where

$$E = \frac{K^2_{max} + K_o^2}{K_{max}} = \frac{K^2_{min} + K_o^2}{K_{min}} \tag{22}$$

III. GENERAL ARRANGEMENT AND PROCEDURE

The physical arrangement of the components used in this experiment is shown in Fig. 3. Targets mounted in the cyclotron may be viewed through windows in the cyclotron tank, and through collimating holes through six feet of lead and fifteen feet of concrete shielding. The center lines of these collimating holes are tangent to the 55-1/2 inch radius and the 80-1/2 inch radius of the circulating beam. Utilizing a small probe, called the junior probe, capable of moving along the tangent line to the 55-1/2 inch radius, targets may be placed at any radius between 55-1/2 inches and 80-1/2 inches, with a particular angle of view to the incident beam for each radius. The following energies and related angles were adopted for this experiment.

Proton Energy	Radius	Angles of View
345 Mev	80-1/2 inches	0°, 47°, 90°, 133°, 180°
285 Mev	72 inches	39°, 141°
240 Mev	65 inches	32°, 148°
185 Mev	55-1/2 inches	2°, 178°

The targets were mounted on an adjustable holder on the junior probe allowing the angle and vertical position to be optimized, and a similar target holder was constructed for the main probe of the cyclotron.

Three settings of the magnetic field were required for each spectrum measured, and for each of these settings a new sandwich target was required to monitor the proton beam. The radiator was adjusted for each field setting to maintain the same scattering losses in the pair spectrometer as shown in section IV, and a close check was maintained of the accidental coincidences to keep corrections to the data from this source

below 5 percent of the total number of events recorded. The length of each bombardment was approximately one hour, which for 345 Mev proton bombardments gave approximately 10,000 recorded events, while for the lower proton energies somewhat less than 1000 events would be recorded for the same bombardment.

IV. ANALYSIS OF PAIR SPECTROMETER

The pair spectrometer used in this experiment is shown in Fig. 4. The gamma radiation is converted into an electron positron pair by the tantalum radiator, the pair then being analyzed by the magnetic field, and detected by the array of geiger tubes backed by pairs of proportional counters. A separate analysis of each of these components follows.

A. Quadruple Coincidence Circuit

Quadruple coincidence from the pairs of proportional tubes are required to reduce the accidental coincidences to a small fraction of the total coincidences detected. The pulses from the proportional tubes are amplified and then formed into 1μ sec. square pulses. These are then fed into a mixing circuit, and double and quadruple coincidences fed into scalers. Simultaneously, the quadruple coincidence pulse is formed into a 1-1/2μ sec. square pulse which is used to make the geiger tube amplifiers sensitive to pulses from the geiger tubes.

B. Geiger Coincidence Matrix

The signals from the geiger amplifiers are fed into a 14 square matrix coincidence circuit. Each geiger tube on the electron side of the pair spectrometer feeds the control grids of a row of coincidence tubes, while each geiger tube on the positron side of the pair spectrometer feeds the

the suppressor grids of a column of coincidence tubes. Therefore an electron positron coincidence results in a pulse in the plate curcuit of the coincidence tube at the intersection of the appropriate column and row. Since the gamma ray energy is the sum of the electron and positron energy all coincidences along a diagonal of the matrix represent a single energy gamma ray. Therefore al outputs of the coincidence tubes on a diagonal are coupled together and fed into a single register channel. Consequently, 27 different energy channels are measured for any one setting of the magnetic field. The gate signal from the proportional tubes is required as the matrix coincidence circuit is extremely slow, requiring 20 millisecond pulses to operate the registers.

C. Detection Efficiency of the Converted Gamma Rays

Fig. 5 is a schematic plot of the energy segment detected by each coincidence tube in the 14 square matrix. The diagonal element of the matrix represents the complete range of pair fraction energy covered by the coincidence circuit for each gamma ray energy, and it is apparent that the main diagonal detects gamma rays corresponding to this energy with considerable more efficiency than any of the short diagonals. An exact calculation of the detection efficiency requires the integration of the expression for pair production probability, as given by Rossi and Greissen,[14] over the range of pair fraction energies detected by each diagonal.

$$\overline{\Psi}(K,U_{max}) = \int_{(1-U_{max})}^{U_{max}} 4\alpha \frac{N}{A} Z^2 r_e^2 \left[U^2 + (1-U)^2 + \frac{2}{3} U(1-U)\right] \left[\log \frac{2K}{\mu_e c^2} U(1-U) - \frac{1}{2}\right] du \tag{23}$$

where K is the gamma ray energy and U is the fraction of gamma ray energy received by the electron. The positron fractional energy would be (1-U).

This expression may be integrated approximately to 0.1 percent by expanding the logarithmic term into an infinite series; the resulting expression for detection efficiency being

$$\overline{\psi}(KV) = \frac{4}{9} \frac{N}{A} z^2 r_e^2 RV(6 + V^2) - 2^3$$

where

$$R = \log \frac{2K}{4\mu_e C^2} - \frac{1}{2} \quad \text{and } V = 2U - 1 \tag{24}$$

The expression is a function of magnetic field setting and of the sum of the electron and positron radii for the particular channel considered. If we normalize the functions to that of the main diagonal, the dependence on H is less than 1 percent and thus the normalized factors are a function only of the pair spectrometer geometry. Fig. 10 is a table of values used in normalizing the data for a 14 square matrix, and a 13 square matrix.

D. Mean Energy of Matrix Channels

The gamma ray energy is determined by the sum of the $H\rho$ of the electron and positron. Since these pairs are created uniformly throughout the tantalum radiator, it is necessary to calculate the average of the sum of these two radii. Refering to Fig. 6A

$$\rho_1^2 = X_1^2 + (\rho_1 - \delta)^2 - 2(\rho_1 - \delta) X_1 \sqrt{2} \tag{25}$$

$$\rho_2^2 = X_2^2 + (\rho_2 + \delta)^2 - 2(\rho_2 + \delta) X_2 \sqrt{2} \tag{26}$$

Therefore we find

$$\rho_1 + \rho_2 = \frac{X_1 + X_2}{\sqrt{2}} \left[1 + \frac{2}{X_1 X_2} \right] \tag{27}$$

Averaging over the entire radiator

$$\overline{\rho_1 + \rho_2} = \frac{X_1 + X_2}{\sqrt{2}} \left[1 + \gamma \right] \tag{28}$$

where

$$\gamma = \frac{1}{X_1 X_2} \frac{1}{W} \int_{-\frac{W}{2}}^{+\frac{W}{2}} \delta^2 d\delta \tag{29}$$

A more complicated case, for the radiator placed at a point off the vertex of the geiger tube lines of centers, as shown in Fig. 6B, shows that

$$\gamma = \frac{\frac{W^2}{12} + m}{X_1 X_2} \tag{30}$$

Now in the coincidence matrix the only requirement for each diagonal is that the sum of x_1 and x_2 be a constant, 2c, and therefore we desire the average value of γ over the acceptable range of values of x_1 and x_2

$$\bar{\gamma} = \frac{\frac{W^2}{12} + m^2}{\Delta c} \int_0^c \frac{dy}{(c+y)(c-y)} = \frac{\frac{W^2}{12} + m^2}{\Delta c} \log \frac{c+\Delta c}{c-\Delta c} \tag{31}$$

where

$$\Delta c = c - x_{min} \text{ for } c < \frac{x_{max} - x_{min}}{2}$$

and

$$\Delta c = x_{max} - c \text{ for } c > \frac{x_{max} - x_{min}}{2} \tag{32}$$

Fig. 7 is a plot of $\overline{\gamma}$ vs. coincidence channels while Table I gives the values of $\overline{\rho_1 + \rho_2}$.

E. Loss of Energy of Electron Radiator

Heitler[15] shows that for high energy electrons the loss of energy in the radiator is given by

$$\frac{dE}{dx} = 4NE \left[\log \frac{2E}{\mu_e c^2} - \frac{1}{3} \right] \frac{r_e^2 Z^2}{137} \tag{33}$$

where r_e is the classical radius of the electron.

For the case of a thin tantalum radiator with electron pairs created uniformly throughout the volume

$$\frac{\overline{\Delta E}}{E} \cong 0.003^t \tag{34}$$

Thus a small correction of the gamma ray energy is required for this loss.

F. Multiple Scattering in Radiator

Rossi and Greissen[14] give the multiple scattering of a charged particle in passing through a radiator as a gaussian pattern with a mean square angle of scatter of

$$\overline{\theta^2} = \frac{1}{2} \overline{\phi^2} = \frac{E_s^2 t}{2\beta^2 c^2 p^2} \tag{35}$$

where θ is the projection of ϕ on a plane, $E_s = 21$ Mev, and t is measured in radiation lengths. For relativistic energies $\beta = 1$ and $cp = E$, therefore

$$\overline{\theta^2} = \frac{21^2}{2E^2} t \tag{36}$$

The horizontal scattering in the radiator has the effect~~ive~~ of broadening

the gamma ray spectra, but for the thin radiator used in this experiment the amount of broadening is completely negligible. However, due to the vertical scattering, the height of the proportional tubes places a serious limitation on the thickness of radiator that one may use.

The fraction of the electrons detected by the spectrometer for any position in the radiator is given by the integral of the gaussian probability function between the limits of the angles subtended by the detector -- see Fig. 8.

$$\mathcal{F} = \frac{2}{\sqrt{\pi}} \int_{x_1}^{x_2} e^{-x^2}\, dx \tag{37}$$

where $x = \theta/\sqrt{\overline{\theta^2}}$.

Since the radiator has a finite height we must integrate this function over the vertical extent of the radiator

$$\overline{\mathcal{F}} = 2 \int_0^{\lambda} \mathcal{F}\, dK \tag{38}$$

where K is measured vertically from center line of radiator. The $\mathcal{F}$ values may be obtained from standard tables, but the integration over the radiator must be done numerically. If one assumes that the limiting angles are determined by the pole faces then the values of the $\overline{\mathcal{F}}$ are as a function of magnetic field and radiator thickness, and the scattering losses would be a constant for the condition that t/H^2 constant. Actually the limiting aperture in the pair spectrometer is the proportional counters, and since these are not located along the lines whose vertex intersects at the radiator, the scattering losses increase for the low energy channels. Fig. 9 shows the detection efficiency for each electron channel for the

particular case of a 0.007 inch radiator, of the same height as the proportional counter, and for a 8510 gauss magnetic field. To reduce the losses in the low energy channels, the radiators used were only 2 inches high while the proportional counter aperture is 3-1/2 inches. Under these conditions the calculated losses due to scattering were less than 2 percent.

V. PROTON BEAM MONITOR

The proton beam is monitored by measuring the activity induced in 0.001 inch aluminum foils sandwiched between layers of carbon targets as shown in Fig. 10. The relation of this activity to the incident beam is given by the $Al^{27}(p,3pn)Na^{24}$ cross section, as measured by P. Stevenson,[16] which is shown in Fig. 11. Two foils in each sandwich make it possible to check on misalignment of the target face with the direction of the incident beam. Since the total activity on the foil is measured, it is essential that the portion of the carbon target exposed to the beam be completely visible to all parts of the radiator in the pair spectrometer. The effects of multiple passage were minimized by using 1/4 inch carbon targets. A plot of the quadruple coincidences per unit target thickness against target thickness is shown in Fig. 12 for a constant proton beam. This would be a flat curve if multiple traversals are not present and a 1/4 inch carbon target satisfies this requirement. A measure of the radial penetration of the beam into the target is shown in Fig. 13 where the activity per unit radial distance vs. radial position is plotted. This indicates that the half-breadth for radial penetration is approximately 1/8 inch and therefore small imperfection in the foil at the target edge would

not cause serious error in the measured activity. Fig. 14 shows the corresponding excitation curves $C^{12}(p,pn)C^{11}$, as measured by Aamodt, Peterson and Phillips,[17] used in the absolute determination of the proton beam exposure with polystyrene foils.

VI. RESULTS AND CONCLUSIONS

The gamma ray spectra, for five angles of view of the target bombarded by 345 Mev Protons, are shown in a linear plot in Fig. ~~14~~ 15. In section II it was shown that the spectra for different angles of view should be symmetric curves, identical in shape, but displaced along the diagonal, when the log of the intensity is plotted against the log of the gamma ray energy, providing the radiation originates solely from a spherically symmetric emission of neutral pions in a unique reference frame. Fig. 16 shows the spectra plotted in this manner and it is immediately evident that they do not fit this criterion. This is not surprising since the observed doppler shift of the spectra indicate a proton-nucleon origin of the radiation, and the assumption of a unique reference frame would not be expected to hold true, due to the internal momenta of the nucleons in the nucleus.

In section II it was also shown that the spectrum obtained by integrating the intensity for each gamma ray energy over all angles of view of the target should be symmetric on a plot of the log of the gamma ray energy, and should be centered about the value of half the rest energy of the neutral pion. Since the observed spectra were for only five angles of view it is necessary to arbitrarily divide the sphere into five zones centered about each of the angles of observation. The weighted average

spectrum obtained by this procedure is shown in Fig. 17, and it is apparent that the spectrum is not centered about the accepted value of the half energy of the neutral pion as measured by Aamodt, Hadley, and Panofsky[12] in the negative pion capture in hydrogen. The discrepancy from symmetry about the 67-1/2 Mev line is not conclusive since the low energy measurements are mose subject to errors other than the statistical errors shown. Since pions interact strongly with matter the reactions

$$\begin{aligned} \pi^- + p &\longrightarrow n + \gamma \\ \pi^+ + n &\longrightarrow p + \gamma \\ \pi^0 + n &\longrightarrow n + \gamma \\ \pi^0 + p &\longrightarrow p + \gamma \end{aligned} \tag{39}$$

may appreciably contribute to the observed gamma ray spectra. The inverse processes have been observed in the photo production of pions, while the direct absorption of pion to form stars indicate considerable energy is carried off by the nucleons. Brueckner, Serber, and Watson[18] show that the mean free path of pions in the nucleus is of the order of

$$\lambda = 2a_0$$

where

$$a_0 = 1.5 \times 10^{-13} \text{cm.} \tag{40}$$

If the pions are produced uniformly throughout the nucleus we would expect the radiation from heavy nuclei to contain a large portion of the non-neutral pion radiation due to greater absorption of the pions formed in the interior of the nucleus. The spectra from tungsten have been measured and compared with carbon and found to be identical in shape. In

addition Hales,[19] Hildebrand, Knable, and Moyer have measured the production of high energy gamma rays from targets bombarded by 340 Mev protons and find that the yield increases as $A^{2/3}$ which would confirm the absorption of neutral pions formed in the interior of the nucleus but discount the emission of high energy gamma radiation following their absorption. This argument is not applicable if the pions are produced on the surface, due to the short mean free paths of the incident protons in nuclear matter.

A further check on radiation from sources other than neutral pion decay is obtained from the measurement of the spectra for lower proton energies. These spectra are shown in Fig. 18. As the energy available for neutral pion production approaches the threshold value, the reduced kinetic energy of the neutral pion results in a smaller doppler shift of the decay gamma radiation and this is reflected in the narrowing of the observed spectra as we approach lower proton energies. In fact, it is necessary for the proton to select nucleons moving opposite to its directions with kinetic energies close to 20 Mev for the available energy to be sufficient for a neutral pion to be produced with protons of 185 Mev energy. Also, since the nucleons are restricted in direction and energy, the approach to a unique center of mass reference frame becomes more pronounced and one would expect much more symmetric curves, and this appears to be born out experimentally. In addition, any radiation originating from radiative capture would be expected to be separated more pronouncedly, due to the narrowing of the spectra, and since this is not observed it does not seem likely that the unknown component of radiation is a large fraction of the observed radiation.

Based on these conclusions it is possible to determine the excitation function for the production of neutral pions in carbon under proton bombardment. No marked divergence from spherical emission of the gamma radiation is noted other than the doppler shift and aberration effects. Therefor the transformation of the spectra for supplementary angle of observation to the center of mass frame, and integration of their intensity over all gamma ray energies should be a measure of the relative yields of neutral pions for each bombarding energy. Finally, an absolute measurement of the proton beam during the measurement of any one of the spectra places the xcitation curve on an absolute scale. The absolute measurement of the beam current was made with 0.001 inch polystyrene foils sandwiched in the carbon targets, and the counter geometry determined by using a standard source. The resulting excitation function is shown in Fig. 19. Brueckner et al., have calculated an excitation function based on psuedo scalar pion with psuedo scalar coupling and a Fermi distribution of nucleon momenta and this curve is also shown in Fig. 19.

Another basic assumption in these measurements is that all the neutral pions decay within the area around the target viewed by the radiator of the pair spectrometer. This is certainly the case since the neutral pion has a lifetime of less than 10^{-13} sec. as shown by the measurements of Carlson et al.,[13] on cosmic ray stars. Measurements were made in conjuction with the work reported here which would set an upper limit on the half life of less than 10^{-12} seconds. The experiment consisted of measurement of the gamma radiation observed as a block of uranium, 1/2 inch thick, was moved in steps of 0.0025 inch across a tungsten ribbon target, 0.010 inch thick in the direction of motion of the uranium block. The block

was placed 3 inches away from the target, while the pair spectrometer was a distance of 600 inches from the target. From strictly geometrical considerations the cutoff of the gamma radiation should have been completed over a range of motion of the uranium block of 0.020 inch. Fig. 20 shows a plot of the actual cutoff as well as the geometrical cutoff. From this one can say that the observed radiation does not originate at distances greater than 0.005 inches from the target, which, on the assumption of neutral pions with velocities approaching that of light as indicated by wide spread in the observed spectra, would mean that these pions had decayed in something less than

$$\Delta T \cong \frac{0.005 \times 2.54}{3 \times 10^{10}} = 5 \times 10^{-13} \text{ sec.} \tag{41}$$

If the spectra observed are entirely due to the decay of neutral pions the energy distribution of the neutral pions can be found by differentiating the average gamma ray spectrum as shwon in section II. Fig. 21 is a plot of the energy distribution of the neutral pions emitted by a carbon target bombarded by 345 Mev protons.

Information concerning the angular distribution of those π^{0}'s emitted with rather large momenta may be obtained from the high-energy portion of the photon spectra observed in various directions from the target. That this is true may be seen from the following considerations.

The energy distribution of the neutral pions emitted in a particular direction may be calculated by treating the gamma ray spectra for this angle as representing a spherical symmetric distribution and applying relation (12). (See Fig. 22) On this basis we find that there is a maximum energy neutral pion emitted. Thus for a gamma ray of energy K we have the following limiting neutral pion energies contributing to the

spectrum.

$$K = \frac{K_o}{\gamma_m(1 - \beta_m \cos \theta_m)} = \frac{K_o}{\gamma(1 - \beta)} \tag{42}$$

where γ_m refers to the maximum pion energy and γ refers to the minimum pion energy capable of making a gamma ray of energy K. Using,

$$\gamma = \frac{T + 2K_o}{2K_o} \tag{43}$$

and

$$\beta = \sqrt{\frac{\gamma^2 - 1}{\gamma^2}} \tag{44}$$

we can solve for θ_m,

$$\theta_m = \cos^{-1} \left[\frac{T_m + T\left(\sqrt{1 + \frac{4K_o}{T}} - 1\right)}{T_m \sqrt{1 + \frac{4K_o}{T_m}}} \right] \tag{45}$$

A plot of θ_m versus neutral pion kinetic energy T, for a maximum neutral pion kinetic energy of 150 Mev is shown in Fig. 23. Thus we see that for higher energy pions the assumption of spherical symmetry is reasonable providing the angular distribution is slowly varying, since pions over a small solid angle contribute to the spectrum observed at any angle. Fig. 24 is a plot of the neutral pion energy distribution for the various angles of observation of the gamma ray spectra, transformed to a reference frame with a $\beta = 0.300$. Figure 25 is a polar plot of the pion distribution and it indicates very strongly that the neutral pions are emitted with a $\cos^2\theta$ dependence. The distribution is relatively insensitive to the reference frame since a change to $\beta = 0.400$ only effects the energy and intensity measurements by about 10 percent.

UCRL 2110

VII. ACKNOWLEDGMENTS

The author wishes to thank Professor Burton J. Moyer and Professor W.K.H. Panofsky for their considerable assistance and contributions to the experiment. Many other people assisted in both the design of the pair spectrometer and in the collection of the data. Doctor Darcy Walker, of Birmingham, and Mr. Kenneth Crowe and Mr. Robert Phillips devoted much time to the development of the 14 square matrix coincidence circuit, which made the rapid collection of data possible. Finally, the cyclotron crew, under Mr. James Vale and Mr. Lloyd Houser, made available large quantities of high energy protons, so necessary to the success of the experiment.

VIII. REFERENCES

1. H. Yukawa. Proc. Phys-Math Soc., Japan, 17, 48 (1935).
2. C. M. G. Lattes, G. P. S. Occhialini, and C. F. Powell. Nature, London, 160, 453, 486 (1947).
3. E. Fermi. Elementary Particles. Yale Press (1951).
4. W. Birnbaum, Smith, and W. Barkas. Private Communication.
5. L. Aamodt, J. Hadley, and W. K. H. Panofsky. Phys. Rev. 81, 565 (1951).
6. E. A. Martinelli and W. K. H. Panofsky. Phys. Rev. 77, 465 (1950).
7. L. M. Lederman, E. T. Booth, H. Byfield, and J. Kessler. Phys. Rev. 83, 685 (1951).
8. N. Nereson and B. Rossi. Phys. Rev. 64, 199 (1943).
9. J. R. Oppenheimer. Phys. Rev. 71, 462 (T) (1947).
10. R. E. Marshak and H. A. Bethe. Phys. Rev. 72, 506 (1947).
11. R. Bjorklund, W. Crandall, B. J. Moyer and H. York. Phys. Rev. 77, 213 (1950).
12. J. Steinberger, W. K. H. Panofsky, and J. Stellar. Phys. Rev. 78, 802 (1950).
13. A. G. Carlson, J. E. Hooper, and D. T. King. Phil. Mag. 41, 701 (1950).
14. B. Rossi and K. J. Greissen. Phys. Rev. 61, 121 (1942).
15. W. Heitler. Quantum Theory of Radiation, Oxford Press.
16. P. Stevenson, Private Communication.
17. L. Aamodt, V. Peterson, and R. Phillips. UCRL-1400
18. K. A. Brueckner, R. Serber, and K. M. Watson, Phys. Rev. 84, 258 (1951).
19. R. Hales, R. Hildebrand, N. Knable, and B. J. Moyer. Private Communication.

TABLE I

MEAN RADIUS AND f FACTORS REQUIRED IN CONVERSION OF COINCIDENCE MATRIX DATA TO GAMMA RAY SPECTRA.

Channel No.	$\overline{\rho_1 + \rho_2}$	$f14$	$f13$
1	14.0	8.70	8.35
2	15.0	4.58	4.37
3	16.0	3.21	3.06
4	17.0	2.52	2.40
5	18.0	2.10	2.00
6	19.0	1.82	1.73
7	20.0	1.62	1.54
8	21.0	1.46	1.40
9	22.0	1.34	1.28
10	23.0	1.25	1.19
11	24.0	1.17	1.11
12	25.0	1.10	1.04
13	26.0	1.05	1.00
14	27.0	1.00	1.12
15	28.0	1.11	1.26
16	29.0	1.25	1.43
17	30.0	1.40	1.64
18	31.0	1.58	1.89
19	32.0	1.80	2.22
20	33.0	2.08	2.66
21	34.0	2.44	3.27
22	35.0	2.92	4.18
23	36.0	3.58	5.70

Note: $f14$ are factors for square matrix. $f13$ are factors for 13 square matrix.

TABLE I (CONT'D)

Channel No.	$\overline{\rho_1 + \rho_2}$	f_{14}	f_{13}
24	37.0	4.58	8.75
25	38.0	6.24	17.90
26	39.0	9.55	
27	40.0	19.50	

IX. FIGURE CAPTIONS

Fig. 1. Lorentz transformation of gamma rays.

Fig. 2. Spherically symmetric neutral pion gamma ray spectrum.

Fig. 3. Plan view of cyclotron.

Fig. 4. Plan view of pair spectrometer.

Fig. 5. Energy plot of 14 square matrix.

Fig. 6. Geometry for mean energy calculation.

Fig. 7. γ terms for mean energy correction.

Fig. 8. Vertical scattering geometry.

Fig. 9. Poor geometry detection efficiency.

Fig. 10. Target dimensions.

Fig. 11. $Al^{27}(p,3pn)Na^{24}$ excitation function.

Fig. 12. Multiple traversal measurement.

Fig. 13. Radial penetration measurement.

Fig. 14. $C^{12}(p,pn)C^{11}$ excitation function.

Fig. 15. Linear plot of 345 Mev gamma spectra.

Fig. 16. Log plot of 345 Mev gamma spectrum.

Fig. 17. Average 345 Mev gamma spectrum.

Fig. 18. Low energy gamma spectra.

Fig. 19. Excitation function for neutral pions.

Fig. 20. Attenuation curve for shadow caster.

Fig. 21. Energy distribution of neutral pions.

Fig. 22. Approximation used in angular distribution calculations.

Fig. 23. Maximum angle for which neutral pion symmetry is assumed.

Fig. 24. Energy distribution of neutral pions for various angles.

Fig. 25. Polar plot of neutral pion distribution.

TRANSFORMATION OF GAMMA RAYS

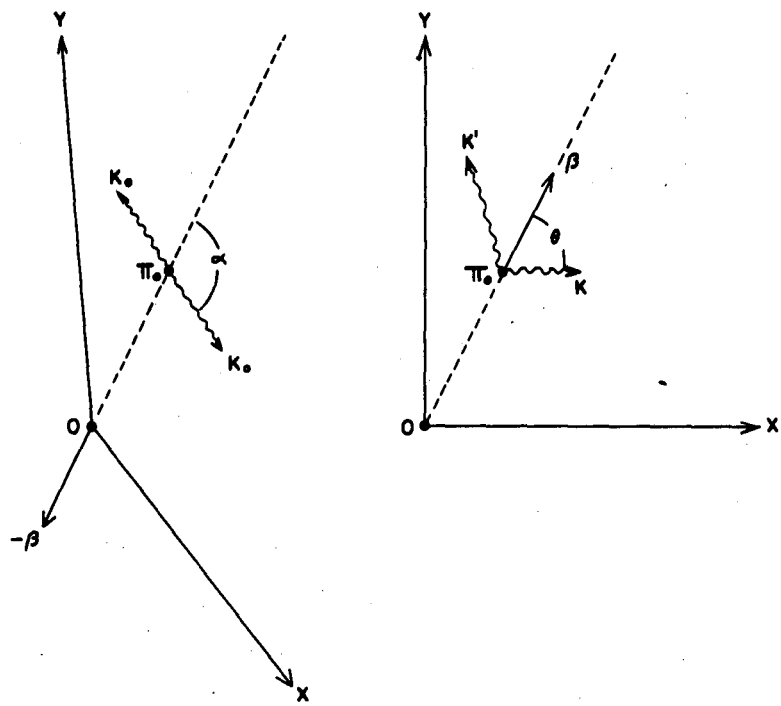

LABORATORY FRAME MOVING $-\beta$
NEUTRAL PION FRAME AT REST

LABORATORY FRAME AT REST
NEUTRAL PION FRAME
MOVING $+\beta$

MU 3136

FIG. 1

SPHERICALLY SYMMETRIC GAMMA RAY SPECTRUM

EACH STEP IS FOR MONOENERGETIC NEUTRAL PIONS OF KINETIC ENERGY T_{π_0}

WHERE $K_{max} K_{min} = K_0^2$

AND $T_{\pi_0} = \frac{(K_{max}-K_0)^2}{K_0} = \frac{(K_{min}-K_0)^2}{K_0}$

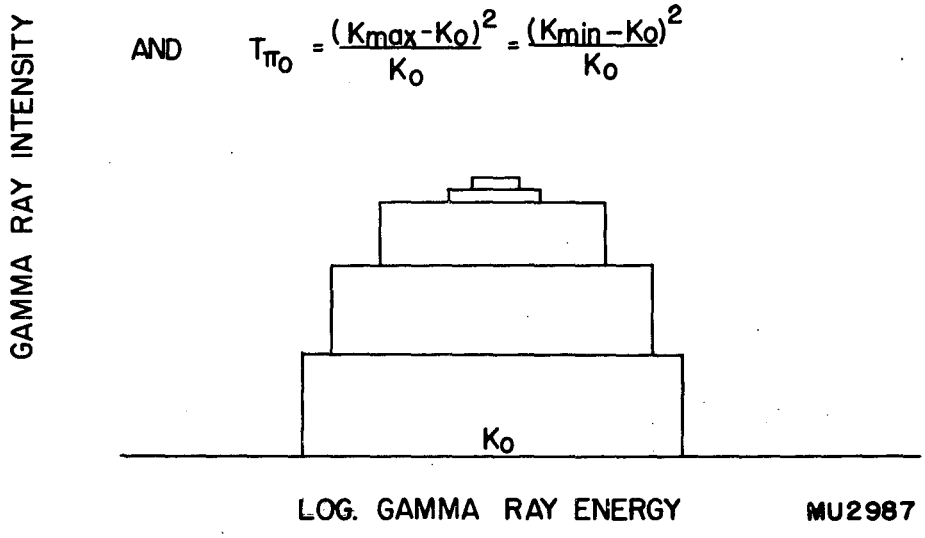

Fig. 2

PLAN VIEW OF CYCLOTRON

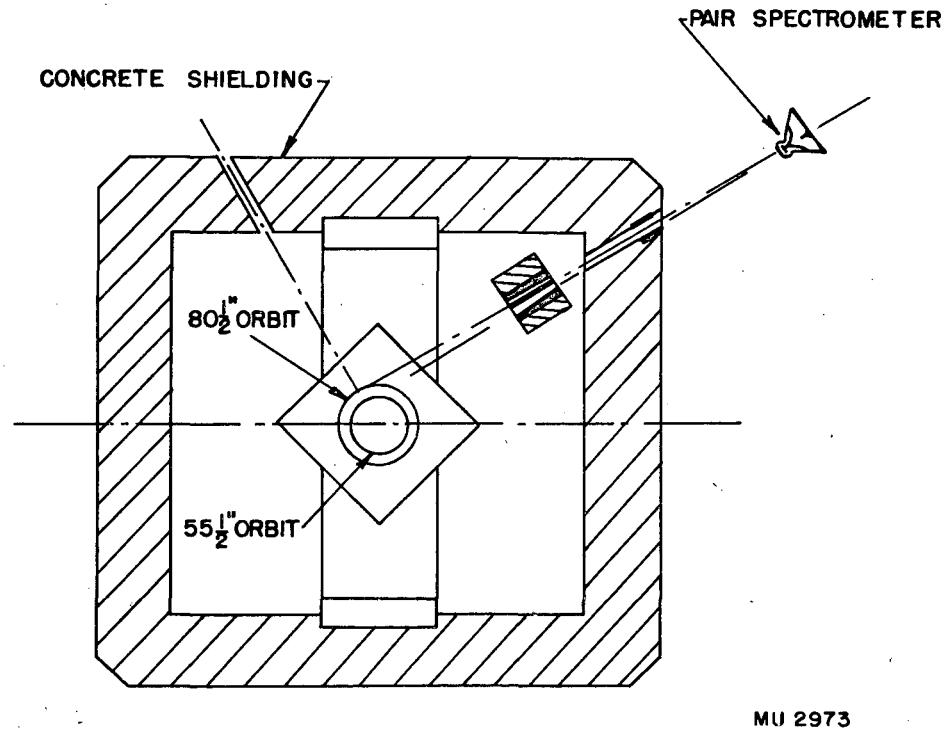

Fig. 3

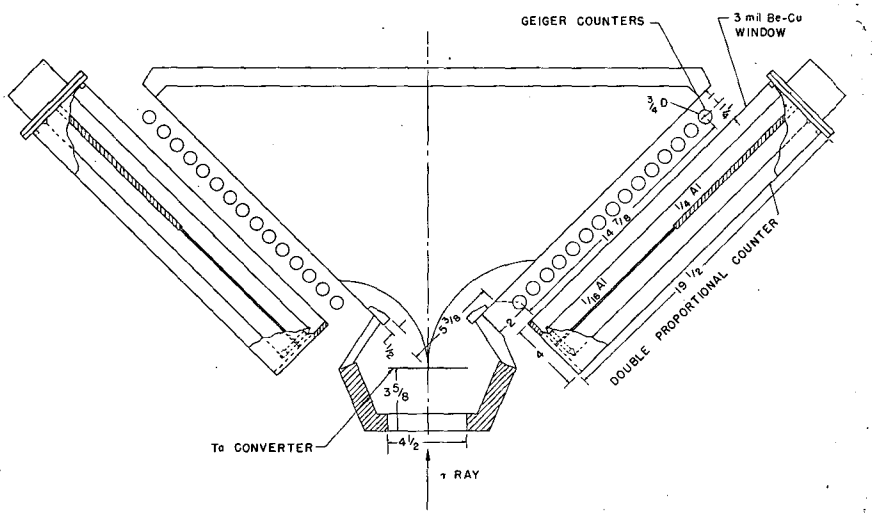
GEIGER COUNTERS
3 mil Be-Cu WINDOW
3/4 D
1/16
1/2 Al
14 7/8
1/16 Al
19 1/2
DOUBLE PROPORTIONAL COUNTER
5 3/8
2
4
1/2
3 5/8
4 1/2
To CONVERTER
γ RAY

Fig. 4

SCHEMATIC PLOT OF 14 SQUARE MATRIX ENERGY PLANE

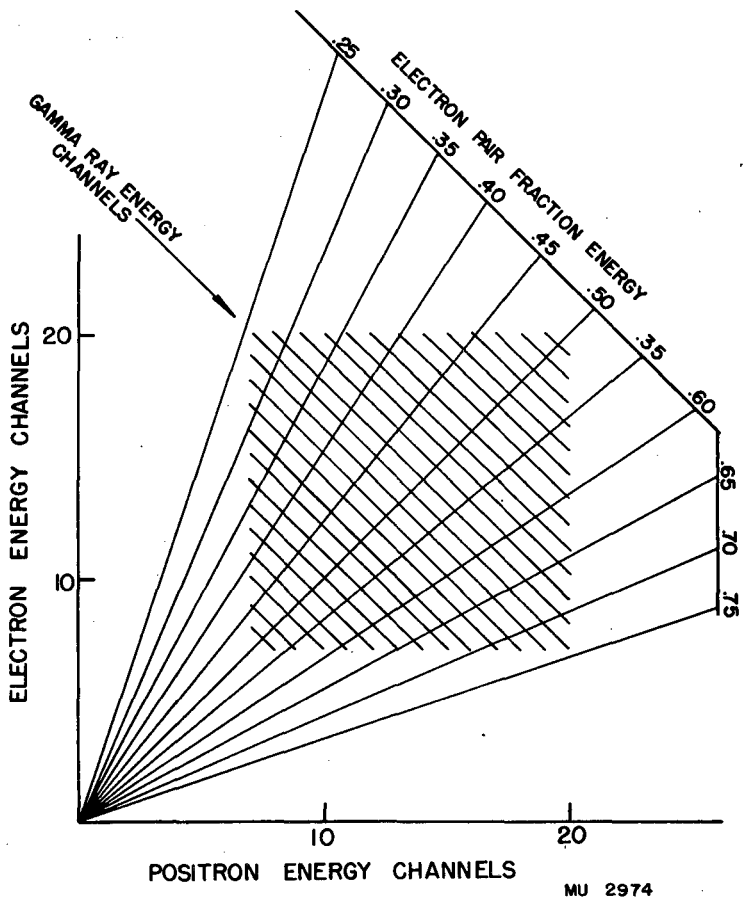

Fig. 5

GEOMETRY FOR MEAN ENERGY CORRECTION

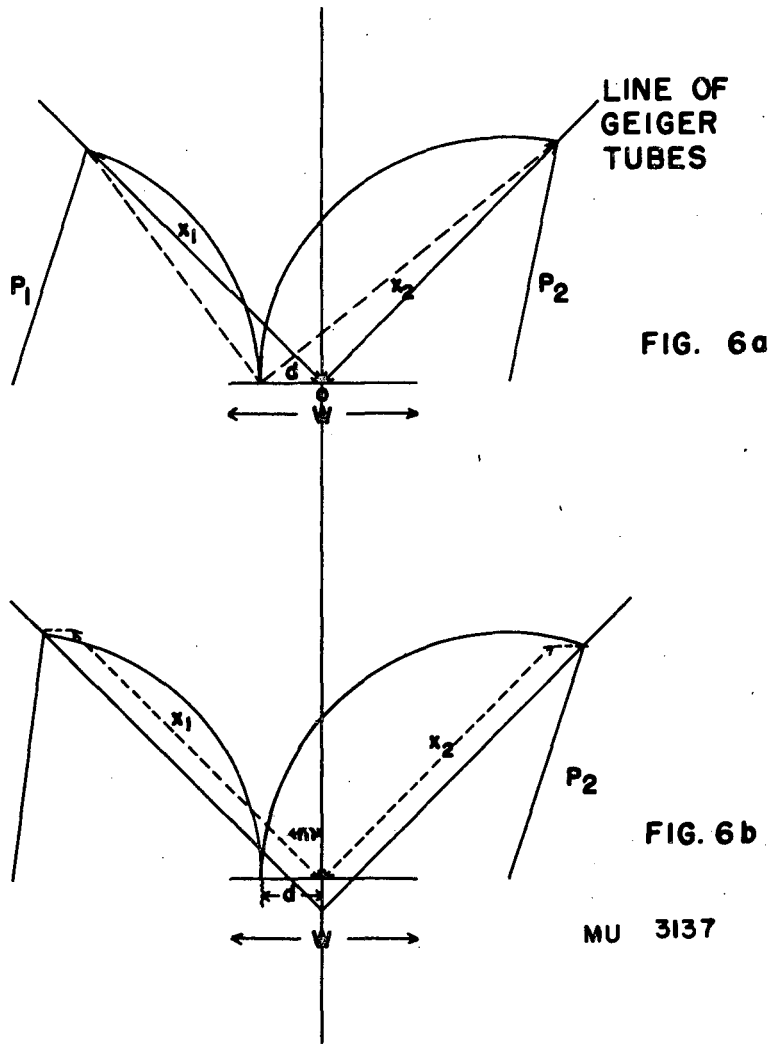

Fig. 6

GAMMA TERM FOR MEAN ENERGY CORRECTION

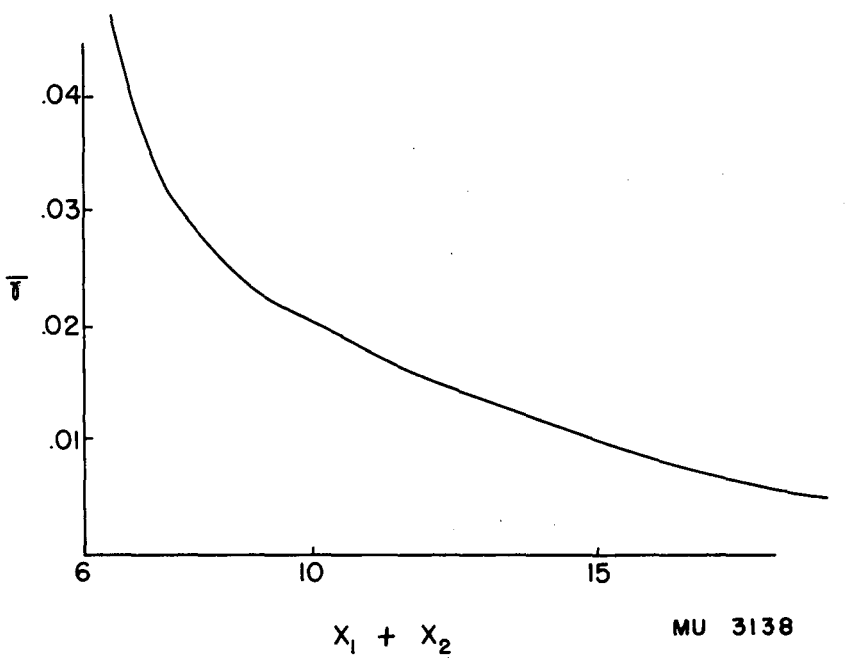

FIG. 7

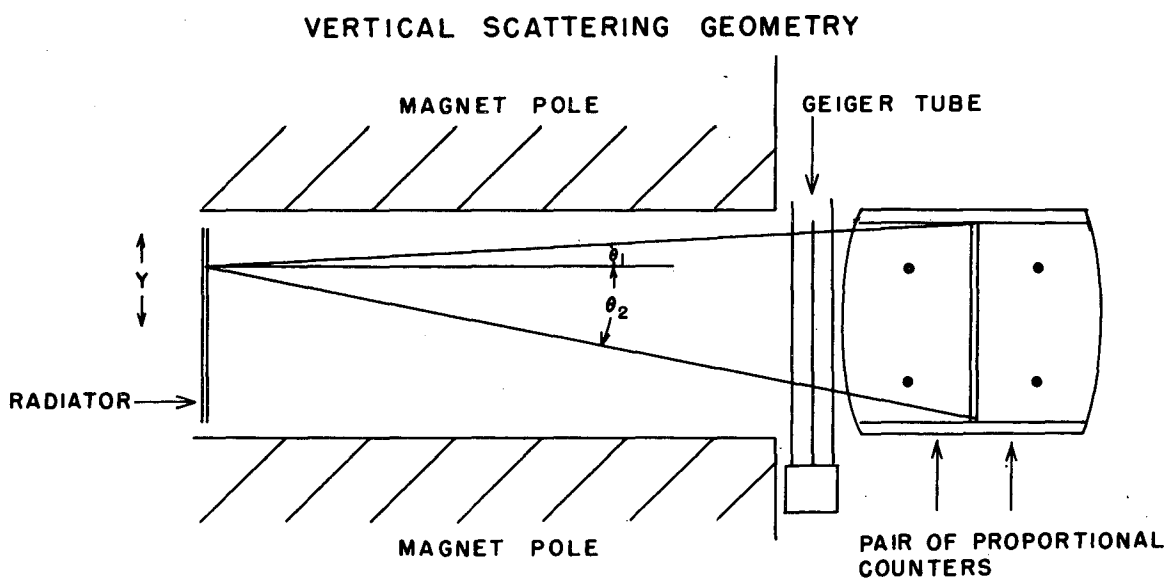

$$X = \sqrt{\frac{\theta}{\theta^2}}$$

MU 3139

FIG. 8

DETECTION EFFICIENCY
FOR CASE OF POOR GEOMETRY

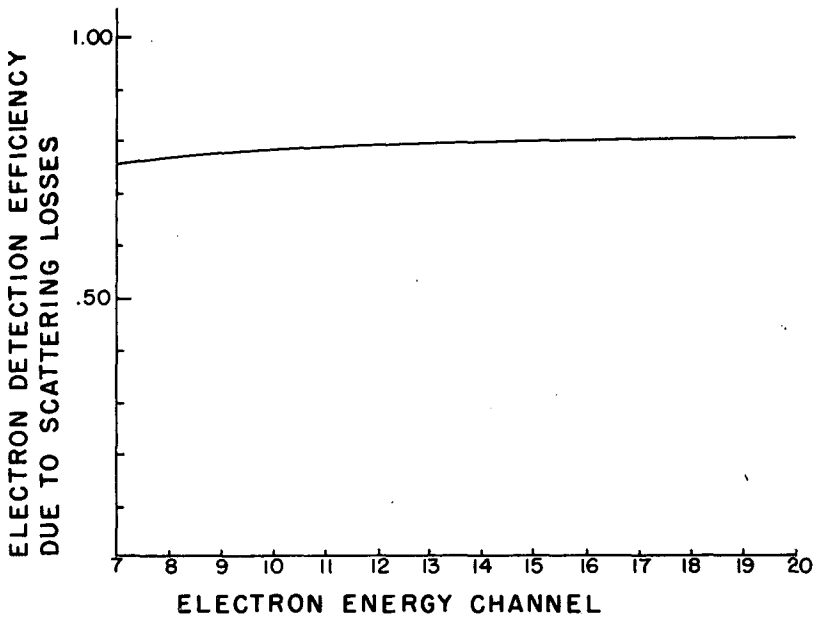

RADIATOR THICKNESS = .007" OF TANTALUM
RADIATOR HEIGHT = 3.5"
PROPORTIONAL TUBE HEIGHT = 3.5"
MAGNETIC FLUX DENSITY = 8510 GAUSS

FIG. 9 MU 3140

TARGET DIMENSIONS

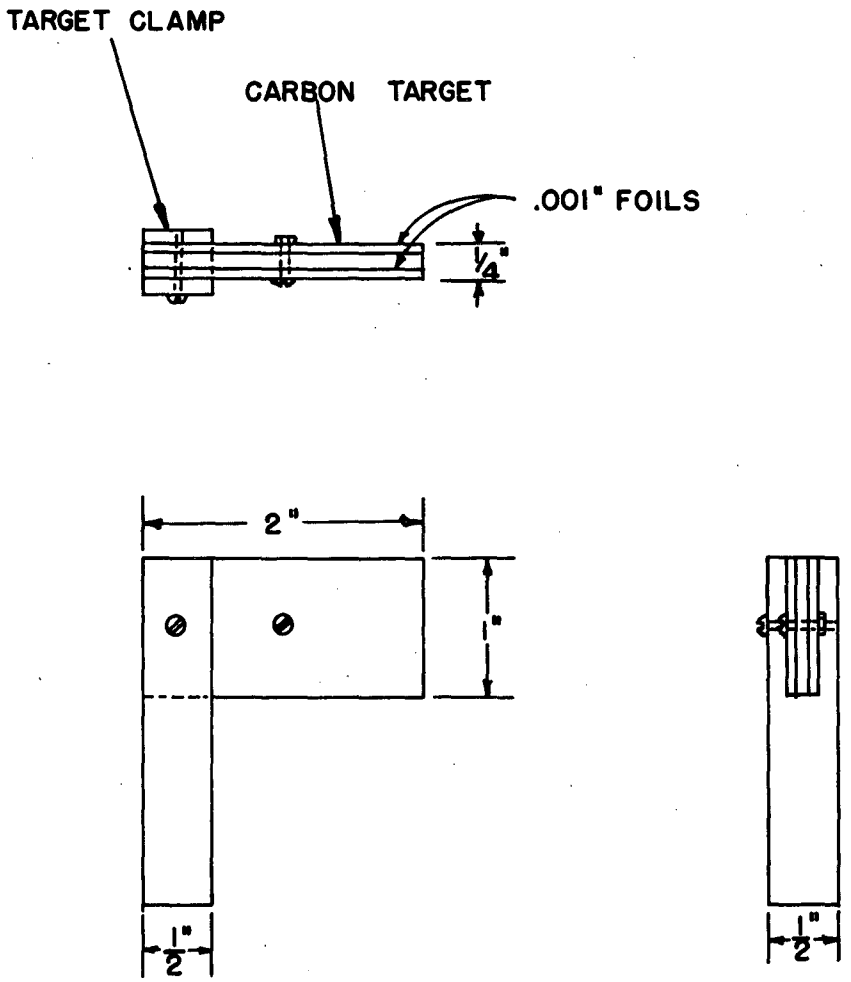

Fig. 10

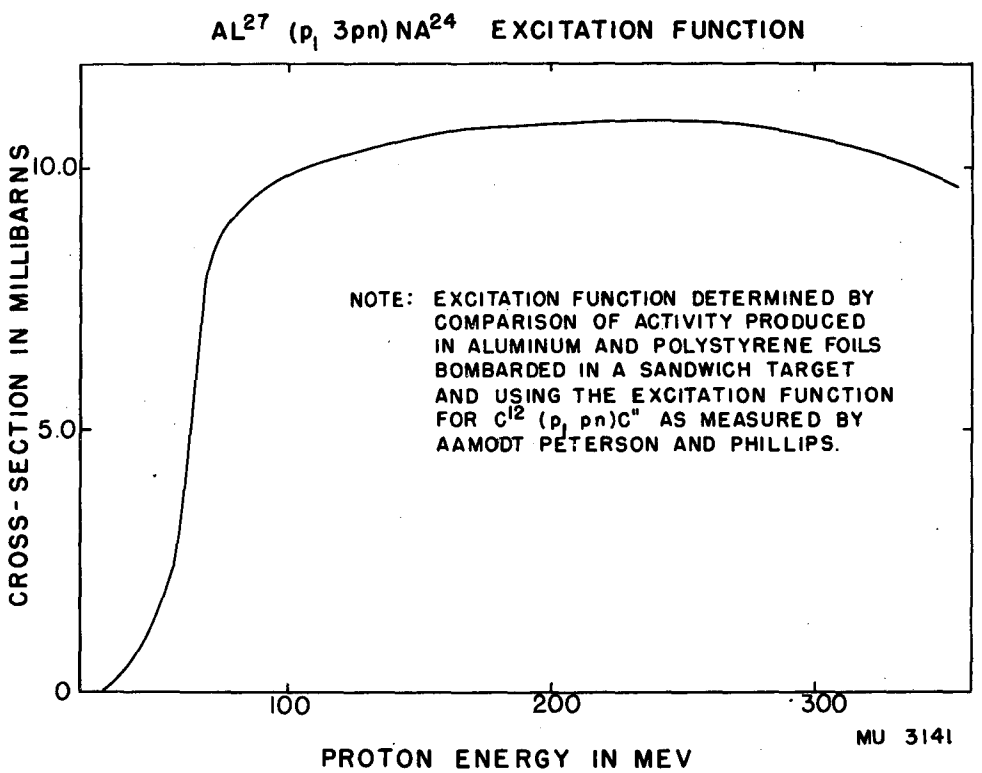
AL27 (p, 3pn) NA24 EXCITATION FUNCTION
CROSS-SECTION IN MILLIBARNS
10.0
5.0
0
100
200
300
NOTE: EXCITATION FUNCTION DETERMINED BY COMPARISON OF ACTIVITY PRODUCED IN ALUMINUM AND POLYSTYRENE FOILS BOMBARDED IN A SANDWICH TARGET AND USING THE EXCITATION FUNCTION FOR C12 (p, pn)C" AS MEASURED BY AAMODT PETERSON AND PHILLIPS.
MU 3141
PROTON ENERGY IN MEV

FIG. 11

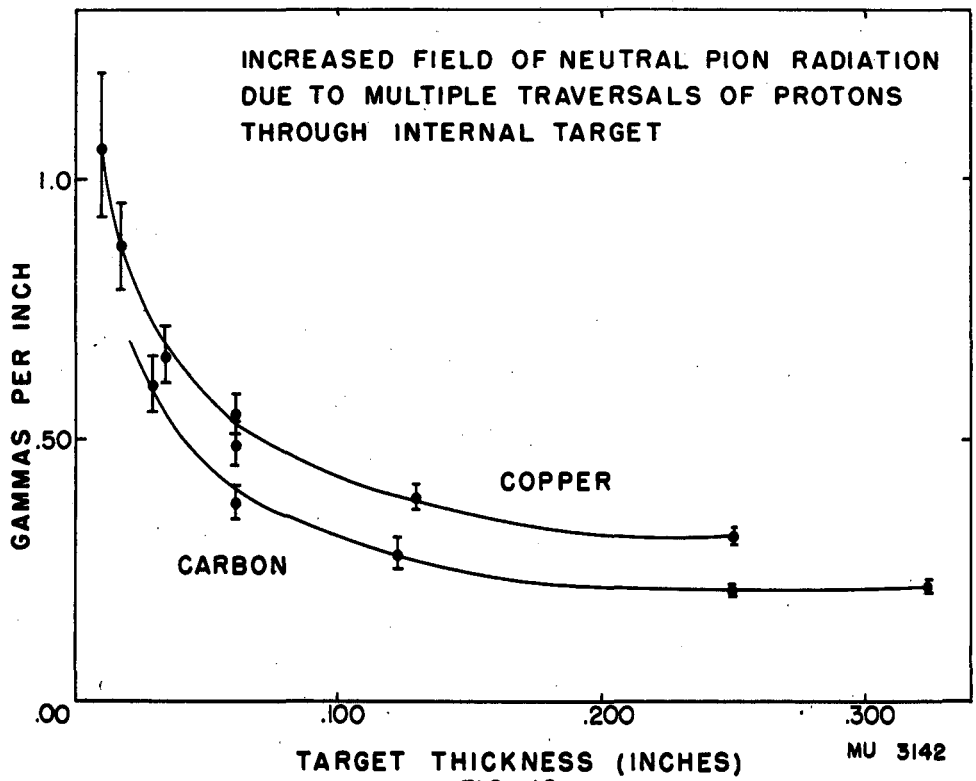
INCREASED FIELD OF NEUTRAL PION RADIATION
DUE TO MULTIPLE TRAVERSALS OF PROTONS
THROUGH INTERNAL TARGET
GAMMAS PER INCH
1.0
.50
.00
.100
.200
.300
COPPER
CARBON
TARGET THICKNESS (INCHES)
MU 3142

FIG. 12

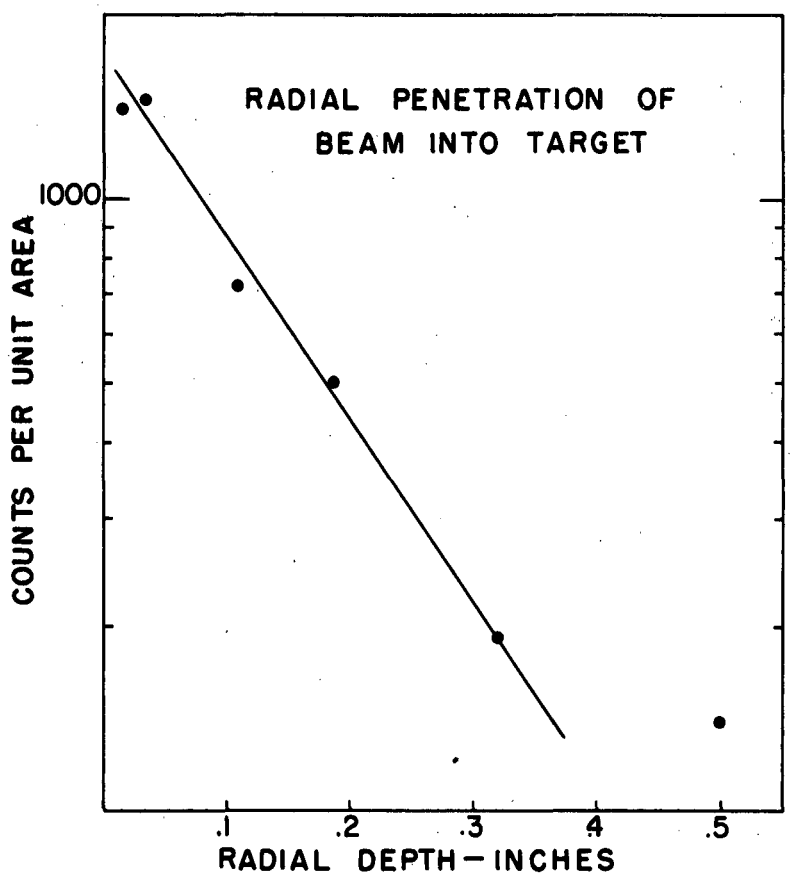

MU 3143

FIG. 13

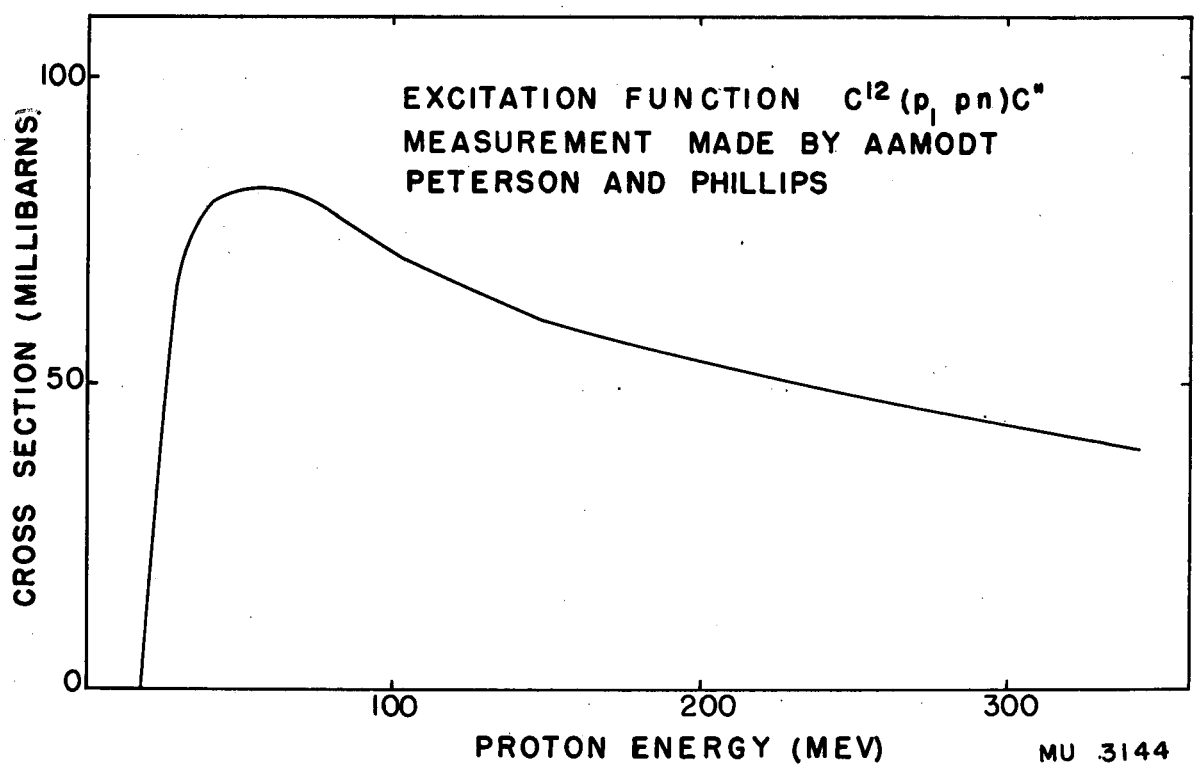
EXCITATION FUNCTION $C^{12}(p, pn)C^{11}$
MEASUREMENT MADE BY AAMODT
PETERSON AND PHILLIPS
CROSS SECTION (MILLIBARNS)
100
50
0
100
200
300
PROTON ENERGY (MEV)
MU 3144

FIG. 14

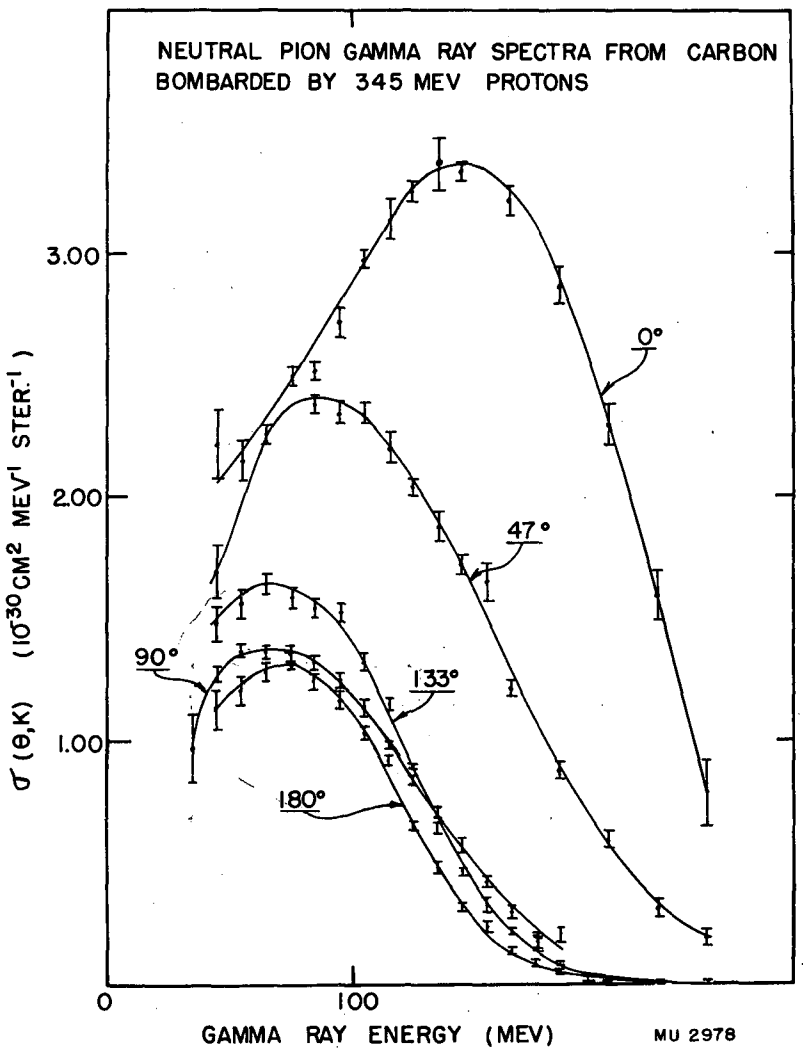
NEUTRAL PION GAMMA RAY SPECTRA FROM CARBON BOMBARDED BY 345 MEV PROTONS
3.00
2.00
1.00
0
100
σ (θ,K) (10⁻³⁰ CM² MEV⁻¹ STER.⁻¹)
GAMMA RAY ENERGY (MEV)
0°
47°
90°
133°
180°
MU 2978

Fig. 15

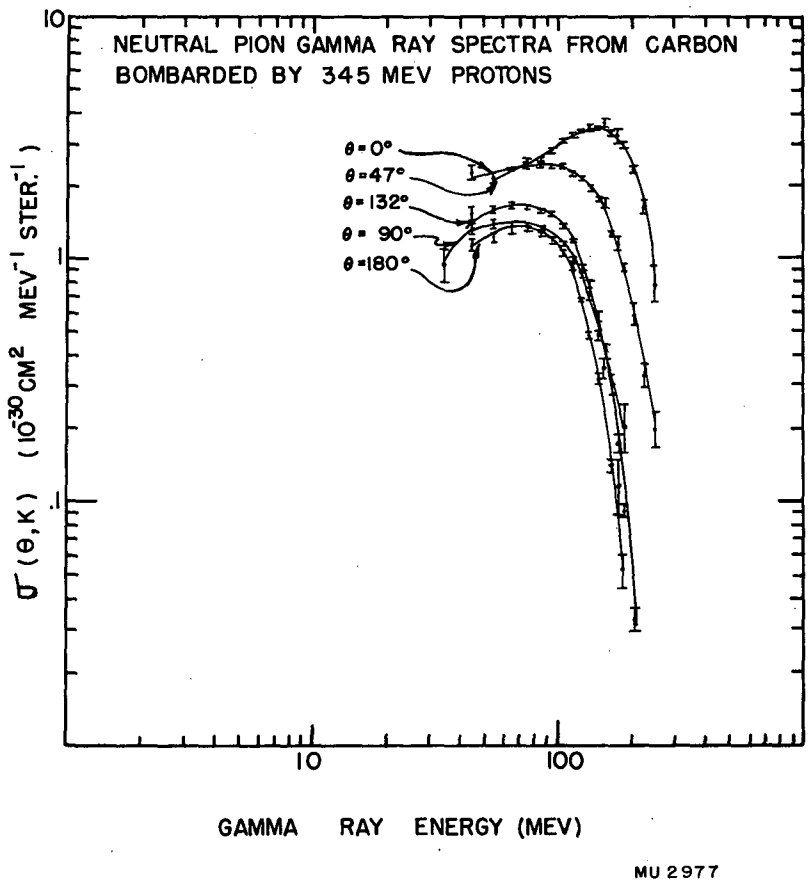
NEUTRAL PION GAMMA RAY SPECTRA FROM CARBON
BOMBARDED BY 345 MEV PROTONS
θ=0°
θ=47°
θ=132°
θ= 90°
θ=180°
10
1
.1
10
100
σ (θ,K) (10⁻³⁰ CM² MEV⁻¹ STER.⁻¹)
GAMMA RAY ENERGY (MEV)
MU 2977

Fig. 16

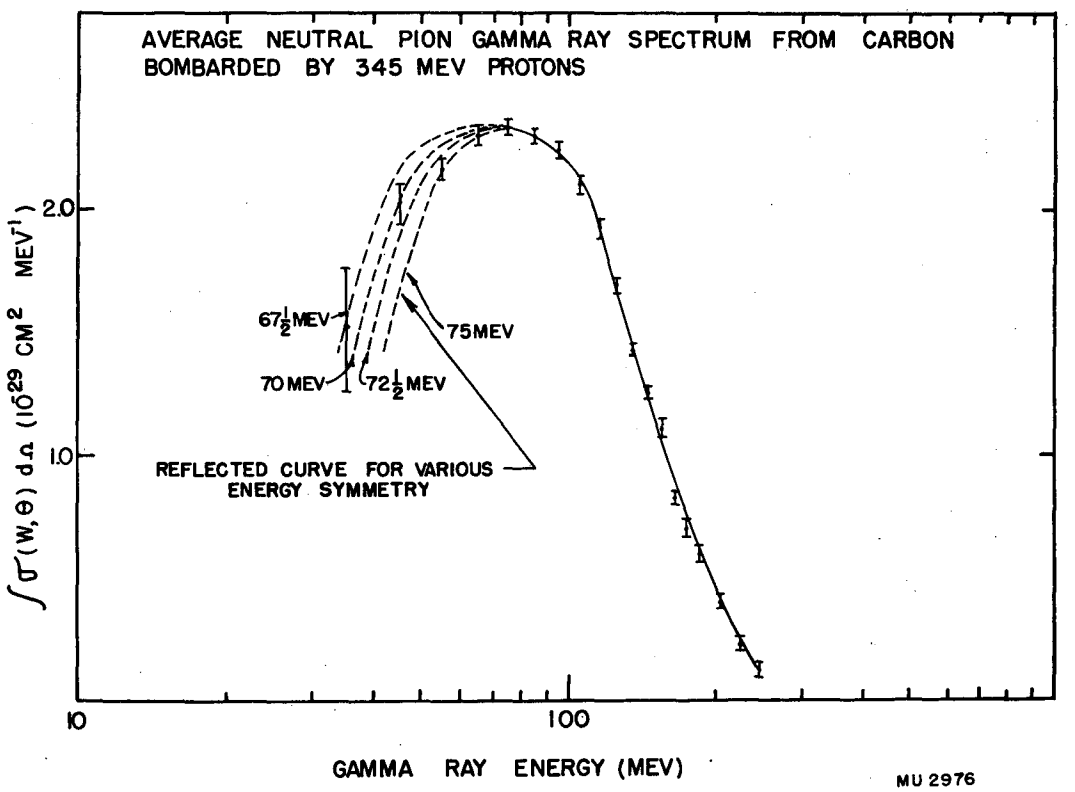
AVERAGE NEUTRAL PION GAMMA RAY SPECTRUM FROM CARBON BOMBARDED BY 345 MEV PROTONS
$\int \sigma(W,\Theta)\, d\Omega\ (10^{-29}\ CM^2\ MEV^{-1})$
2.0
1.0
$67\frac{1}{2}$ MEV
70 MEV
$72\frac{1}{2}$ MEV
75 MEV
REFLECTED CURVE FOR VARIOUS ENERGY SYMMETRY
10
100
GAMMA RAY ENERGY (MEV)
MU 2976

Fig. 17

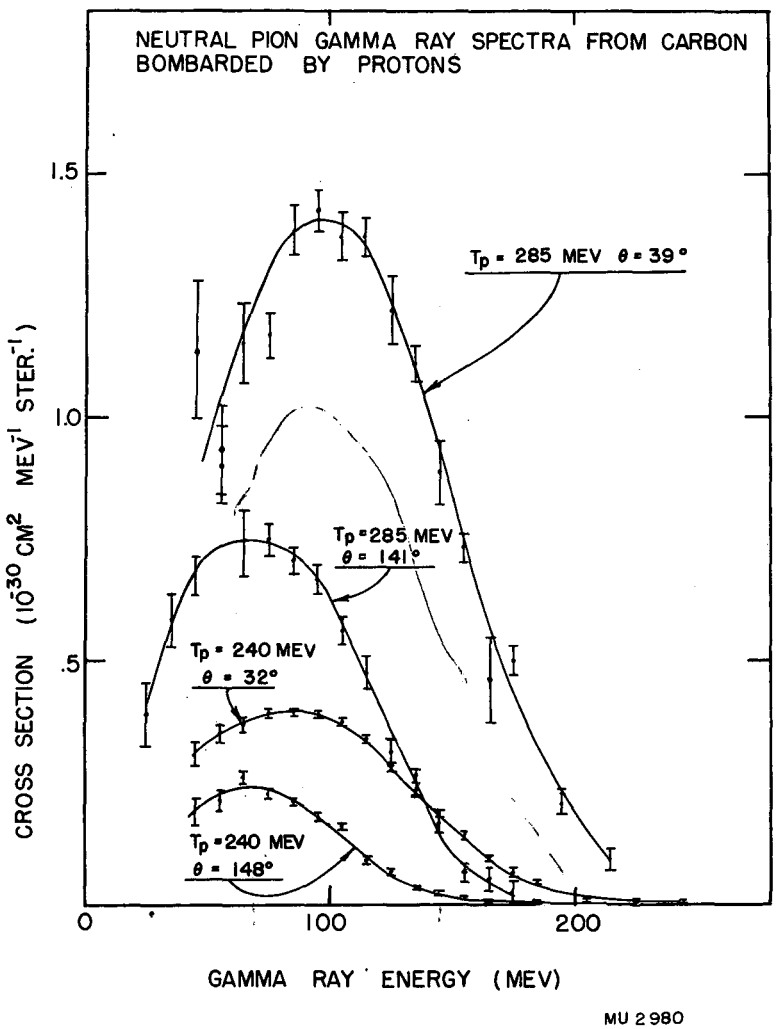
NEUTRAL PION GAMMA RAY SPECTRA FROM CARBON BOMBARDED BY PROTONS
1.5
1.0
.5
0
100
200
CROSS SECTION (10^{-30} CM^2 MEV^{-1} STER.$^{-1}$)
GAMMA RAY ENERGY (MEV)
T_p = 285 MEV θ = 39°
T_p = 285 MEV θ = 141°
T_p = 240 MEV θ = 32°
T_p = 240 MEV θ = 148°
MU 2980

Fig. 18A

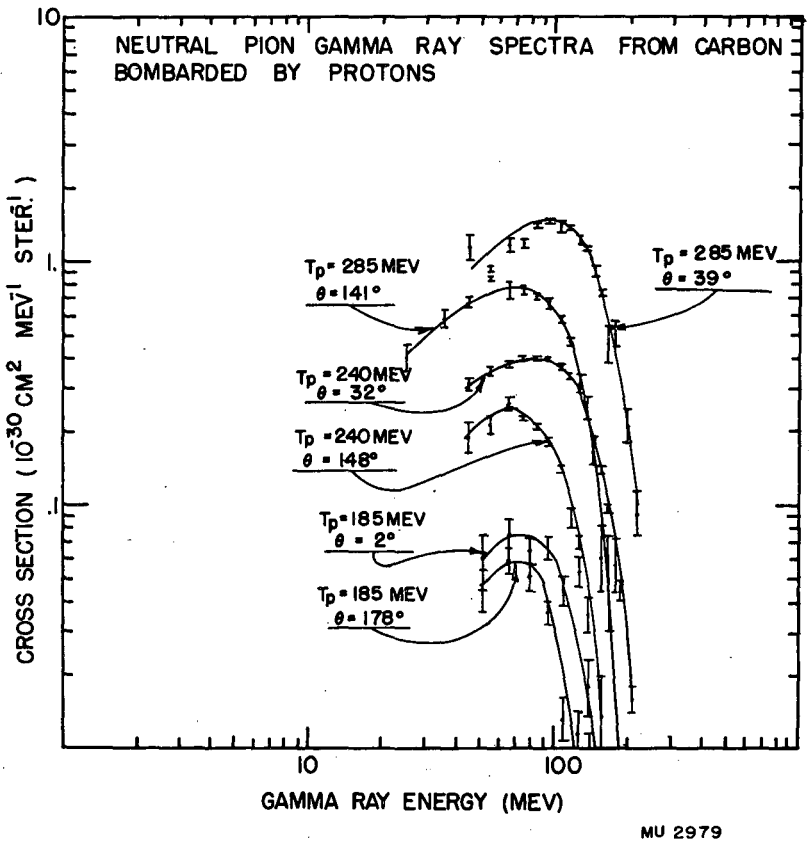
NEUTRAL PION GAMMA RAY SPECTRA FROM CARBON BOMBARDED BY PROTONS
CROSS SECTION (10^{-30} CM^2 MEV^{-1} STER^{-1})
10
1
.1
Tp = 285 MEV
θ = 141°
Tp = 285 MEV
θ = 39°
Tp = 240 MEV
θ = 32°
Tp = 240 MEV
θ = 148°
Tp = 185 MEV
θ = 2°
Tp = 185 MEV
θ = 178°
10
100
GAMMA RAY ENERGY (MEV)
MU 2979

Fig. 18B

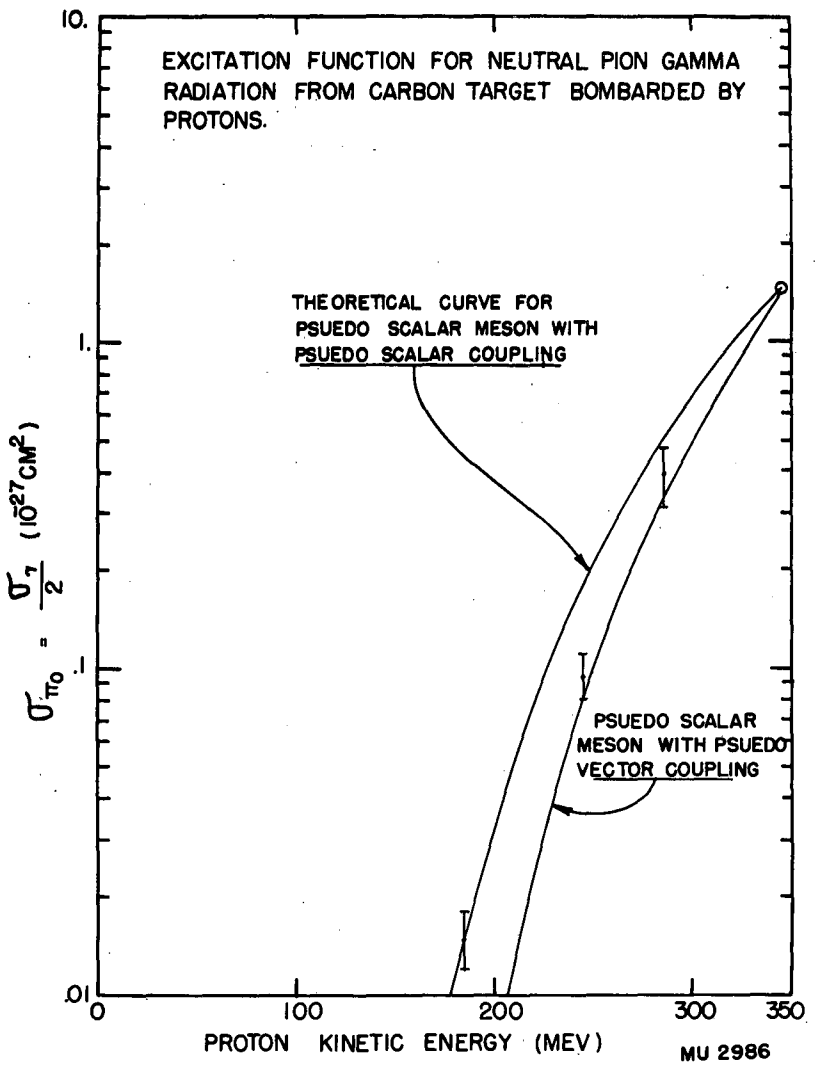
EXCITATION FUNCTION FOR NEUTRAL PION GAMMA RADIATION FROM CARBON TARGET BOMBARDED BY PROTONS.
THEORETICAL CURVE FOR PSUEDO SCALAR MESON WITH PSUEDO SCALAR COUPLING
PSUEDO SCALAR MESON WITH PSUEDO VECTOR COUPLING
$\sigma_{\pi_0} = \frac{\sigma_\gamma}{2}$ $(10^{-27} CM^2)$
10.
1.
.1
.01
0
100
200
300
350
PROTON KINETIC ENERGY (MEV)
MU 2986

Fig. 19

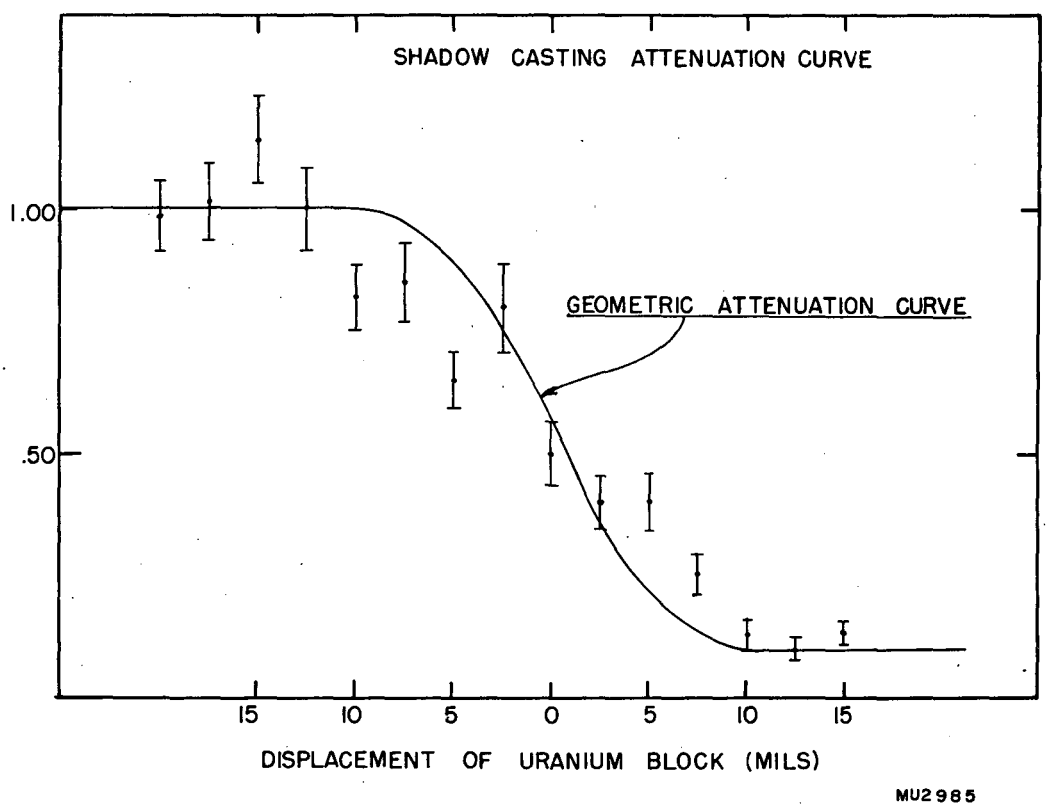
SHADOW CASTING ATTENUATION CURVE
1.00
.50
GEOMETRIC ATTENUATION CURVE
15
10
5
0
5
10
15
DISPLACEMENT OF URANIUM BLOCK (MILS)
MU2985

Fig. 20

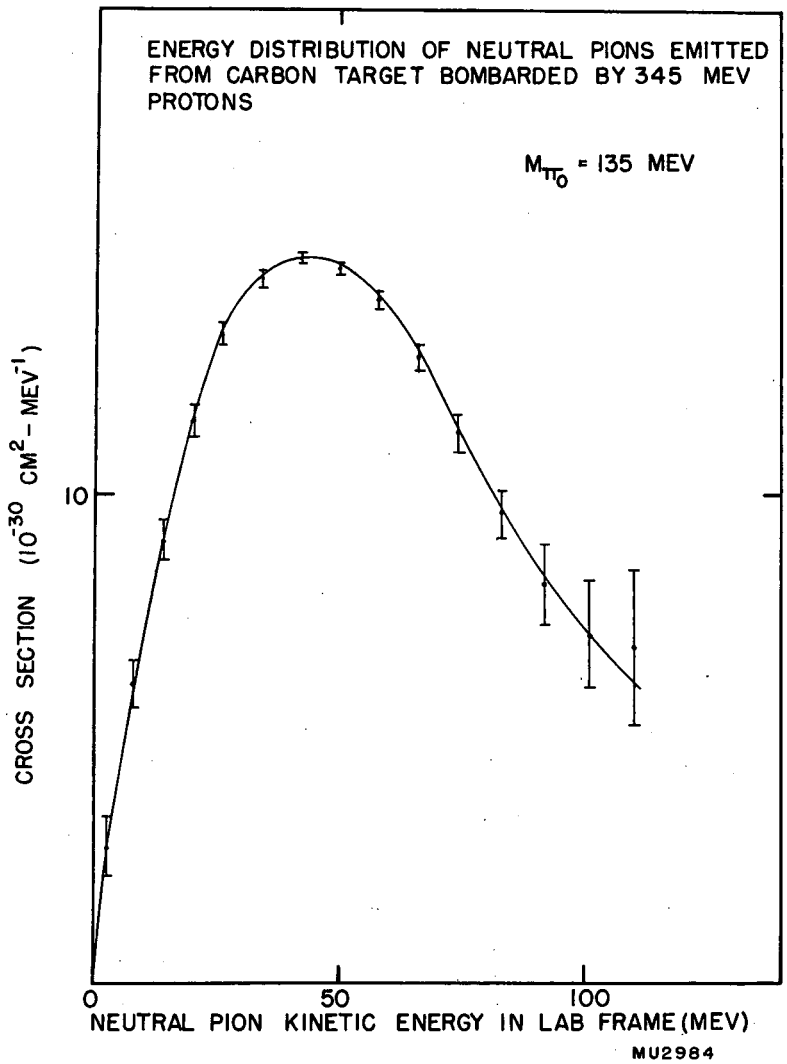
ENERGY DISTRIBUTION OF NEUTRAL PIONS EMITTED FROM CARBON TARGET BOMBARDED BY 345 MEV PROTONS
M_{π_0} = 135 MEV
CROSS SECTION (10^{-30} CM^2 - MEV^{-1})
10
0
50
100
NEUTRAL PION KINETIC ENERGY IN LAB FRAME (MEV)
MU2984

Fig. 21

EXAMPLES OF THE APPROXIMATION USED IN CALCULATING THE ANGULAR DISTRIBUTION OF NEUTRAL PIONS FROM THE MEASURED GAMMA RAY SPECTRA

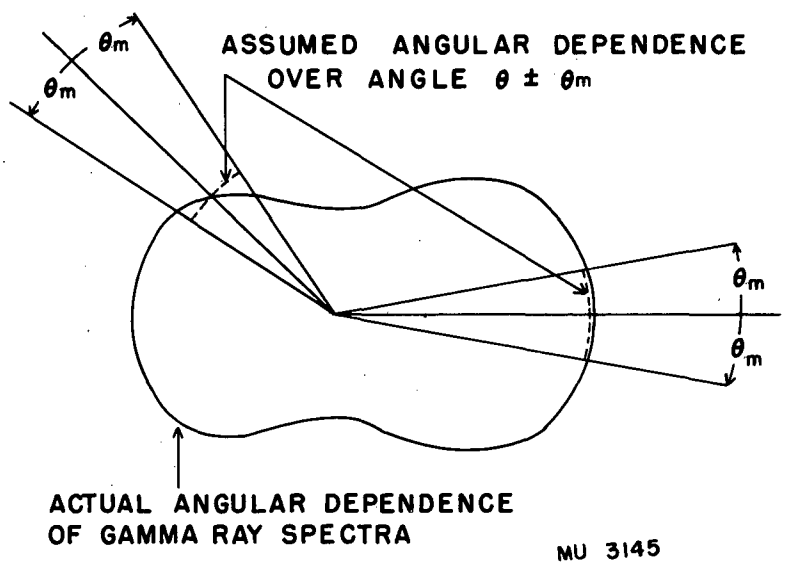

FIG. 22

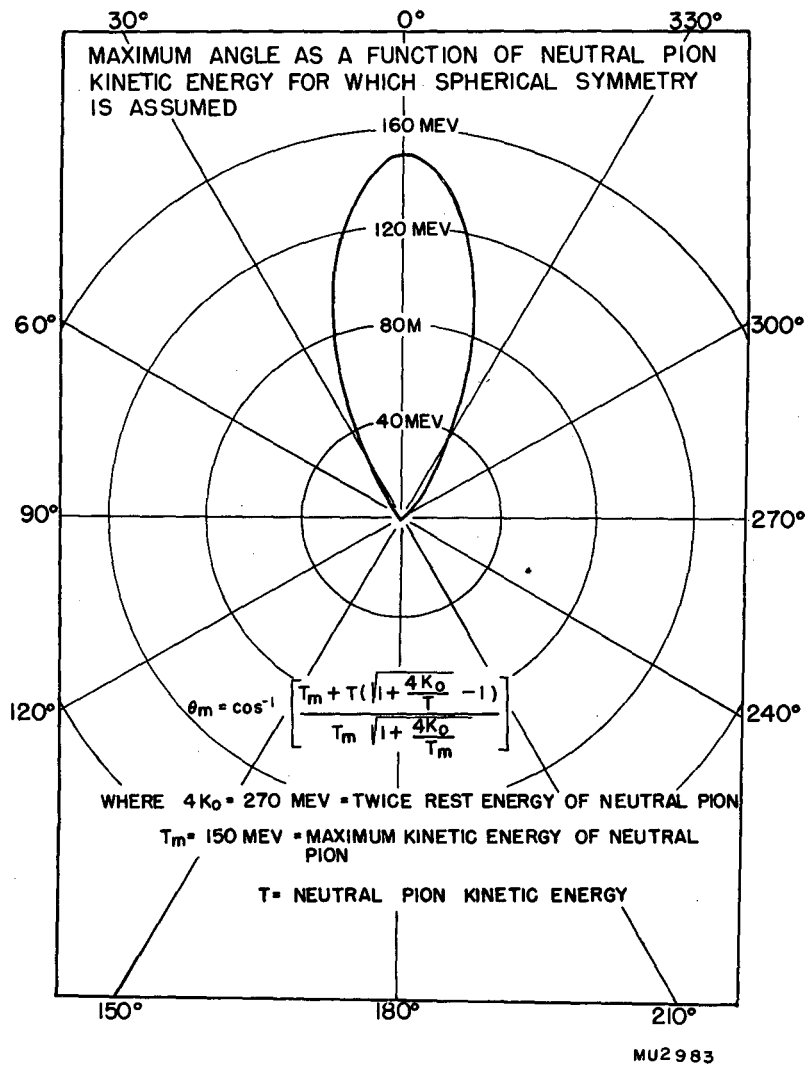
30°
0°
330°
MAXIMUM ANGLE AS A FUNCTION OF NEUTRAL PION KINETIC ENERGY FOR WHICH SPHERICAL SYMMETRY IS ASSUMED
160 MEV
120 MEV
80M
40MEV
60°
300°
90°
270°
120°
240°
$\theta_m = \cos^{-1}\left[\frac{T_m + T\left(\sqrt{1+\frac{4K_o}{T}} - 1\right)}{T_m\sqrt{1+\frac{4K_o}{T_m}}}\right]$
WHERE $4K_o$ = 270 MEV = TWICE REST ENERGY OF NEUTRAL PION
T_m = 150 MEV = MAXIMUM KINETIC ENERGY OF NEUTRAL PION
T = NEUTRAL PION KINETIC ENERGY
150°
180°
210°
MU2983

Fig. 23

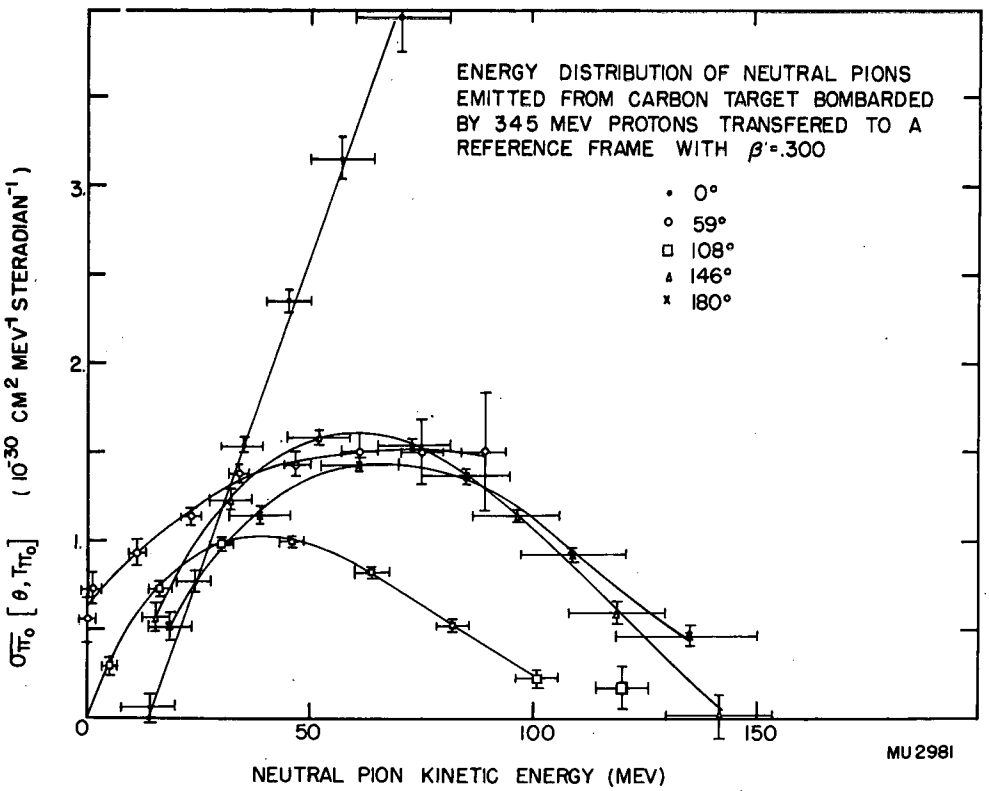
ENERGY DISTRIBUTION OF NEUTRAL PIONS
EMITTED FROM CARBON TARGET BOMBARDED
BY 345 MEV PROTONS TRANSFERED TO A
REFERENCE FRAME WITH β'=.300
• 0°
○ 59°
□ 108°
▲ 146°
× 180°
$\sigma_{\pi_0}[\theta, T_{\pi_0}]$ (10^{-30} CM^2 MEV^{-1} STERADIAN^{-1})
0
1.
2.
3.
50
100
150
MU 2981
NEUTRAL PION KINETIC ENERGY (MEV)

Fig. 24

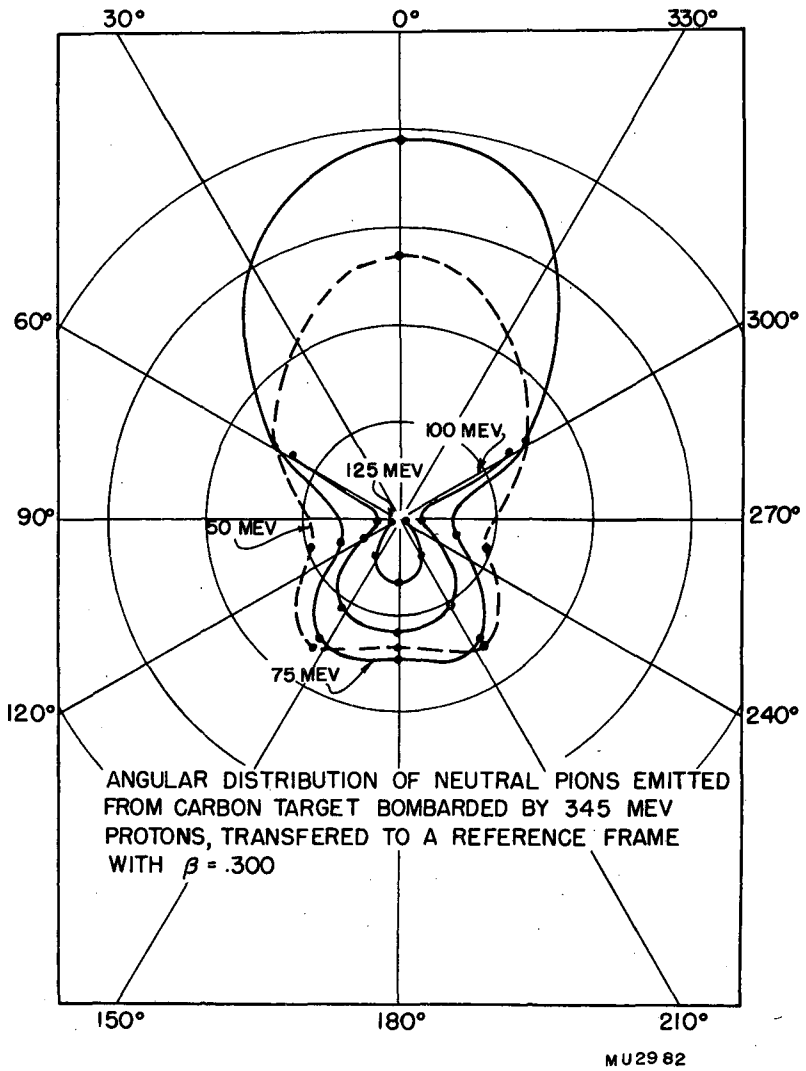
30°
0°
330°
60°
300°
90°
270°
120°
240°
150°
180°
210°
100 MEV
125 MEV
50 MEV
75 MEV
ANGULAR DISTRIBUTION OF NEUTRAL PIONS EMITTED FROM CARBON TARGET BOMBARDED BY 345 MEV PROTONS, TRANSFERED TO A REFERENCE FRAME WITH β = .300
MU2982

Fig. 25